Synthesis of high-T_C ferromagnetic Mn-doped ZnO nanorods by thermal evaporation*

Zheng Kai-Hong(郑凯泓)[a)b)], Liu Zheng(刘 政)[a)b)], Liu Ji(刘 基)[a)b)], Hu Li-Jun (胡丽君)[a)b)], Wang Dong-Wei(王东伟)[a)], Chen Chun-Ying(陈春英)[a)], and Sun Lian-Feng(孙连峰)[a)†]

[a)] *National Center for Nanoscience and Technology, Beijing* 100190, *China*
[b)] *Graduate School of the Chinese Academy of Sciences, Beijing* 100049, *China*

(Received 23 April 2009; revised manuscript received 2 June 2009)

This paper reports that a large amount of Mn-doped ZnO nanorods have been synthesized through thermal evaporation. The morphologies and properties are studied with x-ray diffraction, a scanning electron microscope, transmission electron microscope and Raman spectroscope. The results indicate that the manganese atoms occupy the zinc vacancies in the wurtzite lattice of ZnO without forming secondary phases. The exact manganese content has been studied by the x-ray fluorescence spectrum. Meanwhile, the magnetic moment versus temperature result proves that the as-prepared Mn-doped ZnO nanorods show ferromagnetic properties at temperatures as high as 400 K. These studies provide a good understanding of the origin of magnetic properties in diluted magnetic semiconductors.

Keywords: nanorod, ferromagnetism, Mn-doped ZnO

PACC: 6146, 7550P, 7000

1. Introduction

Diluted magnetic semiconductors (DMS), which combine ferromagnetism with semiconductivity, are envisioned to be potential building blocks for spintronic devices such as spin field-effect transistors, non-volatile memory devices, and quantum computers.[1−5] The II–VI DMS and especially ZnO-based DMS have attracted great interest as it was theoretically predicted that ferromagnetism might exist at room temperature by doping with Mn.[6] Although there are several reports that the Mn-doped ZnO thin film was successfully synthesized, inconsistencies still exist in these reports.[7,8] For example, Deka *et al.*[7] observed paramagnetism at room temperature; Jung *et al.*[8] obtained ferromagnetism with a Curie temperature (T_C) of 45 K; Sharma *et al.*[9] achieved ferromagnetism with a T_C above 420 K. Understanding the origins of magnetic properties in thin films has emerged as one of the great challenges in the magnetism of DMS.[8,9]

In the meantime, the investigations of one-dimensional (1D) Mn-doped ZnO such as nanowires and nanorods are of great interest owing to their unique and fascinating properties as well as their potential applications in nanodevices.[10,11] Generally speaking, there are two approaches for obtaining the 1D Mn-doped ZnO. One is doping the as-synthesized samples by ion implantation,[12] which is a physical method and usually results in a depth variation in doping concentration. The other is incorporating doping elements in the precursors during the growth process.[13−15] It shows the advantages of easy controlling and a uniform doping. However, the experiments should be carried out properly in order to incorporate the doping element into the lattice of ZnO.

Here, we report the growth of Mn-doped ZnO nanorods through thermal evaporation. The x-ray diffraction (XRD), x-ray fluorescence (XRF) and high-resolution transmission electronic microscope (HRTEM) are used to examine the single-crystalline structure of the as-prepared sample. The results confirm that the Mn atoms have been doped into the lattice of ZnO nanorods. The magnetization hysteresis loop and magnetism-temperature data show ferromagnetism with the T_C above 400 K for our Mn-doped ZnO nanorods.

2. Experimental details

A (111) silicon wafer is used as the starting substrate. Before the growth of ZnO nanorods, the sub-

*Project supported by "973" Program of Ministry of Science and Technology of China (Grant No. 2006CB932402) and National Natural Science Foundation of China (Grant Nos. 50702015, 10574034 and 10774032).
†Corresponding author. E-mail: slf@nanoctr.cn
© 2010 Chinese Physical Society and IOP Publishing Ltd

strate is cleaned with acetone, ethanol, and deionized water and a layer of 20 nm Au is deposited as the catalyst. A mixture with a molar ratio of 20:1 of pure Zn (99.9%) and $MnCl_2$ powders (99.5%) is introduced into the middle of the quartz boat. Then, the quartz boat is placed in a horizontal quartz tube downstream, which is evacuated by a mechanical pump and purged with a constant oxygen flow of 1 standard cubic centimeter (SCCM).[16,17] The pressure of the quartz tube is kept constant at 1×10^{-2} Torr (1 Torr = 133 Pa) during the experiment. At last, the temperature of the furnace is increased to 650 °C with an increasing rate of 30 °C/min and maintained for an hour. After the furnace is cooled to room temperature, a layer of light-gray products was visible on the surface of the silicon in the quartz boat.

Phase identification and degree of crystallinity of the as-prepared samples are studied by a D/MAX 2200 VPC x-ray diffractometer with Cu Kα radiation using normal θ–2θ scanning mode. The morphology of the nanorods is studied using a Hitachi S-4800 scanning electron microscope (SEM) and Tecnai G^2 20 ST HRTEM. The XRF analysis (Shimadzu XRF-1800) is used to determine the content of manganese. Raman scattering measurement is performed on a Renishaw 2000 microlaser Raman system at backscattering geometry using the 633 nm line of an Ar^+ laser as excitation source. The magnetic properties of the samples are studied by using a physical property measurement system (Quantum Design PPMS-9).

3. Results and discussion

Figure 1 shows the XRD profiles of ZnO and Mn-doped ZnO nanorods. Compared to the ZnO sample, no manganese-related phases are detected in the Mn-doped ZnO nanorods. For as-grown Mn-doped ZnO nanorods, the main peak corresponding to ZnO (002) is observed, indicating that the Mn-doped ZnO nanorods are preferentially oriented in the C-axis direction. The expanded XRD patterns in the 33.7°–35.5° 2θ region, shown in the inset, clearly indicate that the (002) peak is shifted to lower 2θ values after the doping of ZnO with Mn. As the ionic radius of Mn^{2+} (0.66 Å, 1 Å = 0.1 nm) is larger than that of Zn^{2+} (0.60 Å), the incorporation of Mn will lead to an expansion of the ZnO lattice.[18] Since there is only wurtzite phase in Mn-doped ZnO of the XRD patterns, the doping manganese atoms should substitute the zinc atoms, which result in the shift of (002) peak of ZnO. It is worth while to note that the small peak at 38.1° corresponds to that of Au (111).

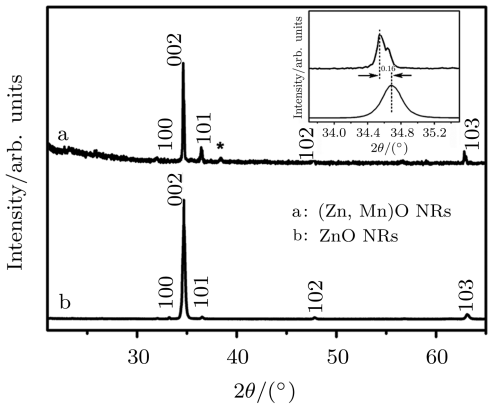


Fig. 1. The XRD patterns for ZnO and (Zn, Mn) O nanorods. The inset shows an expanded view around the ZnO (002) peak. There is a shift of 0.16°. Note the asymmetric shape of the (002) peak of (Zn, Mn) O nanorods comparing to that of ZnO nanorods. (*)Au (111).

Figure 2(a) shows the morphology of Mn-doped nanorods. Most nanorods are straight with length/width ratio larger than 10, revealing that the growth of Mn-doped ZnO nanorods is highly orientated. The diameter and length of the nanorods are in the 50–200 nm range and a few micrometers, respectively. Figures 2(b) and 2(c) show one typical TEM and HRTEM images of the nanorods with diameter around 50 nm. We can see clearly from Fig. 2(c) that the lattice is well aligned without lattice distortion, confirming that Mn-related phases do not form in the nanorods.

The content of Mn in the samples is first studied by energy dispersive x-ray (EDX) spectroscopy. No signal of manganese is found (not shown here), indicating that the content of Mn is below the detection limit of EDX spectroscopy (about 2 at.%). And the exact content of Mn is investigated with the XRF, which has a higher detection limit of 0.01 at.%. In the XRF experiment, the signals of Si and Zn are identified as Kα and Kβ which correspond to different energy level transition of the electrons. Molybdenum (Mo) is used as the anodic target in the XRF test and the related signals are signed by the arrows. In the XRF spectrum (Fig. 2(d)), the typical Mn peak can be clearly observed, further confirming that the Mn atoms are doped into the ZnO nanorods. The exact content of Mn in the samples is found to be 1.38 at.% by XRF, which is consistent with that of EDX result.

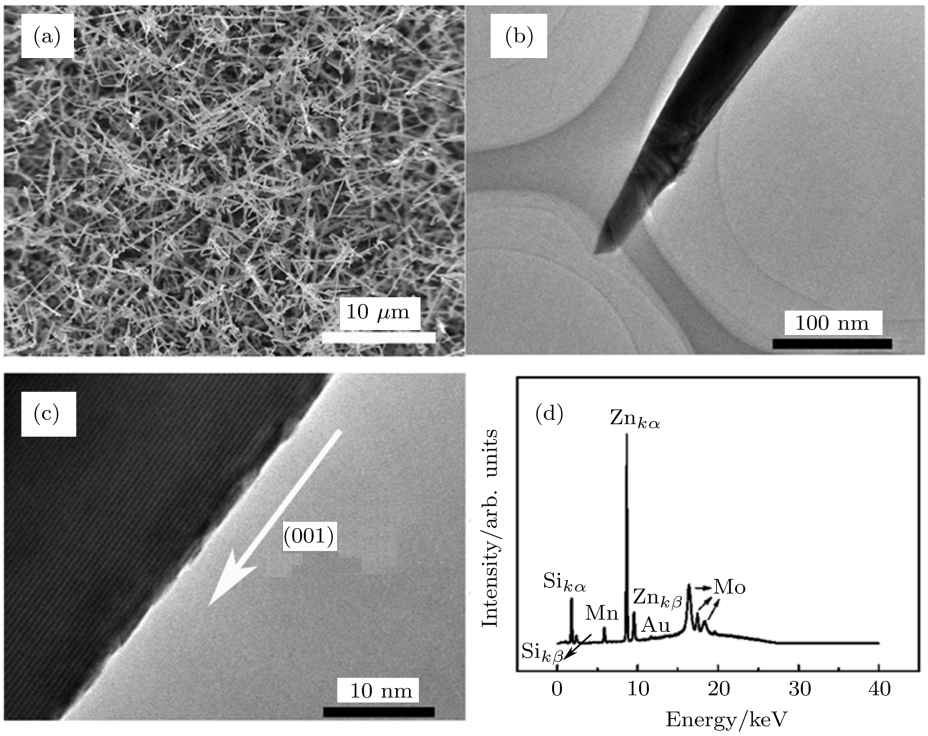


Fig. 2. (a) SEM images showing large scale synthesis of (Zn, Mn) O nanorods. (b), (c) TEM and high-resolution TEM image of an individual (Zn, Mn) O nanorod. (d) Typical XRF spectrum of (Zn, Mn) O nanorods. The peaks of Si and Mo originate from substrate and target. The content of Mn is estimated to be 1.38 at.%.

To disclose the influence of Mn doping on the vibrational property, we investigate the Raman scattering of the ZnO/Mn-doped ZnO nanorods at room temperature. The Raman spectra ranging from 200 cm^{-1} to 700 cm^{-1} are shown in Fig. 3. The sharpest and strongest peak at about 437 cm^{-1} can be assigned to the high frequency branch of $E_2^{\rm high}$ mode of ZnO, which is the main Raman mode in wurtzite crystal structure. Besides, for pure ZnO, the 381 cm^{-1} is $A_1^{\rm TO}$ mode and the 331 cm^{-1} frequency is the second-order vibration mode.[19] In bulk ZnO, only E_2 and A_1 modes can be observed in the Raman spectra according to the selection rule. When the size of ZnO is reduced to nanoscale, the first-order Raman scattering is relaxed and the phonon dispersion around the Brillouin zone center must also be considered. This is the reason why the second-order vibration mode at 331 cm^{-1} can be observed. The broad shoulder centered at about 660 cm^{-1} is thought as originated from two-phonon process.[20] Since Yang *et al.*[21] observed a similar vibration mode at 522 cm^{-1} and considered to be associated with new lattice defects as a result of the doping of Mn, the peak at 523 cm^{-1} can be attributed as an Mn related additional mode.

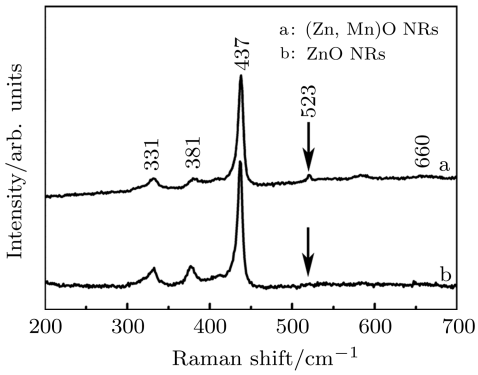


Fig. 3. The comparison between Raman spectra of ZnO and (Zn, Mn) O nanorods. The peak at 523 cm^{-1} in Raman spectra of (Zn, Mn) O nanorods and its absence in ZnO nanorods indicates the successful doping of Mn into the lattice of ZnO. The wavelength of laser is 633 nm.

Magnetic moment of the Mn-doped ZnO nanorods was measured as a function of magnetic field (M–H) and temperature (M–T). Figure 4(a) shows magnetic moment of Mn-doped nanorods at 2 K and 300 K respectively. The distinct hysteretic magnetization loops indicate that Mn-doped ZnO nanorods are ferromagnetic with a characteristic coercive field ($H_{\rm C}$) of 50 Oe (1 Oe = 1 Gb/cm). Figure 4(b) shows the

temperature dependence of the magnetic moment of the Mn-doped ZnO nanorods under a magnetic field of 1000 Oe. The M–T curve is obtained by performing field cooled magnetization measurements at the temperature range of 2–400 K. It can be observed that the magnetic moment decreases rapidly in the temperature range of 2–75 K and very slowly afterwards in the temperature range of 75–400 K. This indicates that the temperature has a great effect towards the magnetic order and results in a temperature-dependent behaviour of magnetization. The magnetic moment at 400 K is about 75% of that at 2 K, which indicates that the Curie temperature of the Mn-doped ZnO nanorods is higher than 400 K (the temperature limit of PPMS-9).

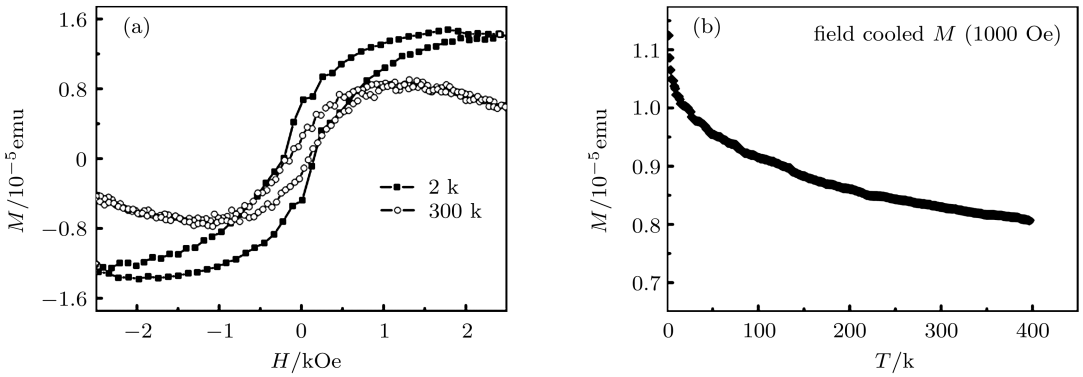


Fig. 4. (a) Magnetic moment hysteresis loop of (Zn, Mn) O nanorods at 2 K and 300 K. (b) M–T curve in an applied field of 1000 Oe of (Zn, Mn) O nanorods sample.

Higher concentration doping of thin film[8] and nanowires[15] with Mn about 10% has been reported previously. The T_C is 30 K for thin film and 37 K for nanowire, respectively, which is much lower than room temperature. This is attributed to be the results of forming the cluster of Mn and consequent antiferromagnetic ordering.[8,15] As shown above, the T_C is above 400 K with a lower doping of Mn about 1.38% in our Mn-doped ZnO. This indicates that although T_C is closely related to the concentration of the dopant, it is important to have a proper concentration to obtain Mn-doped ZnO with higher T_C. From our experiment and a previous study (T_C = 350 K),[10] the concentration of Mn should be about 1% in order to obtain doped ZnO with T_C higher than room temperature.

The origin of ferromagnetism in oxide DMSs is a crucial problem that needs to be explained.[22,23] Experimental works based on iron-doped or cobalt-doped oxides suggest the ferromagnetism resulting from the precipitate of magnetic clusters or secondary magnetic phases.[24,25] Theoretical calculations prove that the origin of ferromagnetism in oxide DMSs are based on the magnetic order which is related to the exchange interaction.[26,27] More recently, it is found that intrinsic defects also play an important role in the magnetic origin for DMSs.[28−30]

It is important to point out that the ferromagnetic behaviour of the Mn-doped ZnO nanorods above room temperature is not arised from the formation of nanoscale Mn-related secondary phases such as MnO, MnO_2, Mn_2O_3, and Mn_3O_4 as reported previously[10] for the following reasons. Firstly, the Curie temperature of Mn_3O_4 is 43 K, and MnO, MnO_2, and Mn_2O_3 are antiferromagnetic materials with Néel temperatures of 116, 92, and 76 K, respectively.[8] Secondly, these Mn-related phases have not been observed in XRD patterns and the (002) peak of ZnO is shifted toward a lower angle by 0.16° with Mn doping, indicating a lattice expansion in Mn-doped ZnO nanorods. Thirdly, no nanoscale phases have been found in HRTEM images. Moreover, the content of Mn in our sample is much lower than that of Mn-containing nanostructures, which is around 10%.[15] Theoretical work indicates that when the Mn concentration is above about 8%, the nearest neighbour interactions become relevant and the Mn substitution cannot result in ferromagnetic behaviour.[27] According to the calculations of density functional theory by Sluiter *et al.*,[31] electron doping with Zn interstitials enhances the ferromagnetic properties of Mn-doped

ZnO. Therefore, the uniform distribution of Mn in ZnO can realize the long-range Mn^{2+}–Mn^{2+} ferromagnetic coupling mediated by itinerant electrons and the room-temperature ferromagnetism behaviour in our Mn-doped ZnO nanorods.

4. Conclusions

In summary, a large amount of Mn-doped ZnO nanorods have been synthesized by thermal evaporation using a mixture of Zn and $MnCl_2$ powders in Ar and O_2 atmosphere. No secondary magnetic phases or lattice distortion have been found in the nanorods. The purity of as-grown Mn-doped ZnO nanorods is estimated to be around 99% according to the results of the XRD, XRF, Raman and M–T curve. The growth of Mn-doped ZnO nanorods is high orientated and the as-prepared Mn-doped ZnO nanorods show ferromagnetic properties at room temperature and at temperatures as high as 400 K. The room-temperature ferromagnetism of the Mn-doped ZnO nanorods originates from the substitution of zinc atoms with Mn atoms and the resulting long-range Mn^{2+}–Mn^{2+} ferromagnetic coupling. These Mn-doped ZnO nanorods offer opportunities for investigations in fundamental science and may also be useful for the development of future nanoscale spintronic semiconductor devices.

References

[1] Furdyna J K 1988 *J. Appl. Phys.* **64** R29
[2] He X B, Yang T Z, Cai J M, Zhang C D, Guo H M, Shi D X, Shen C D and Gao H J 2008 *Chin. Phys.* B **17** 3444
[3] Wolf S A, Awschalom D D, Buhrman R A, Daughton J M, Von Molnár S, Roukes M L, Chtchelkanova A Y and Treger D M 2001 *Science* **294** 1488
[4] Nakayama Y, Pauzauskie P J, Radenovic A, Onorato R M, Saykally R J, Liphardt J and Yang P D 2007 *Nature* (London) **447** 1098
[5] Wang Z L 2007 *Mater. Today* **10** 20
[6] Dietl T, Ohno H, Matsujura F, Cibert J and Ferrand D 2000 *Science* **287** 1019
[7] Deka S and Joy PA 2007 *Solid State Commun.* **142** 190
[8] Jung S W, An S J, Yi G, Jung C U, Lee S and Cho S 2002 *Appl. Phys. Lett.* **80** 4561
[9] Sharma P, Gupta A, Rao K V, Owen F J, Sharma R, Ahuja R, Guillen J M O, Johansson B and Gehring G A 2003 *Nature Mater.* **2** 673
[10] Baik J M and Lee J L 2005 *Adv. Mater.* **17** 2745
[11] Liu X C, Zhang H W, Zhang T, Chen B Y, Chen Z Z, Song L X and Shi E W 2008 *Chin. Phys.* B **17** 1371
[12] Baik J M, Jang H W, Kim J K and Lee J L 2003 *Appl. Phys. Lett.* **82** 583
[13] Wang Y S, Thomas P J and Brien P O 2006 *J. Phys. Chem.* B **110** 21412
[14] Kulkarni J S, Kazakova O and Holmes J D 2006 *Appl. Phys.* A **85** 277
[15] Chang Y Q, Wang D B, Luo X H, Xu X Y, Chen X H, Li L, Chen C P, Wang R M, Xu J and Yu D P 2003 *Appl. Phys. Lett.* **83** 4020
[16] Zheng K H, Zhao Y C, Deng K, Liu Z, Sun L F, Zhang Z X, Song L, Yang H F, Gu C Z and Xie S S 2008 *Appl. Phys. Lett.* **92** 213116
[17] Liu G T, Zhao Y C, Zheng K H, Liu Z, Ma W J, Ren Y, Xie S S and Sun L F 2009 *Nano Lett.* **9** 239
[18] Zhang X M, Zhang Y, Wang Z L, Mai W J, Gu Y D, Chu W S and Wu Z Y 2008 *Appl. Phys. Lett.* **92** 162102
[19] Samanta K, Dussan S, Katiyara R S and Bhattacharya P 2007 *Appl. Phys. Lett.* **90** 261903
[20] Wang J B, Huang G J, Zhong X L, Sun L Z, Zhou Y C and Liu E H 2006 *Appl. Phys. Lett.* **88** 252502
[21] Yang L W, Wu X L, Huang G S, Qiu T and Yang Y M 2005 *J. Appl. Phys.* **97** 014308
[22] Kundaliya D C, Ogale S B, Lofland S E, Dhar S, Metting C J, Shinde S R, Ma Z, Varughese B, Ramanujachary K V, Salamanca R L and Venkatesan T 2004 *Nature Mater.* **3** 709
[23] Behan A J, Mokhtari A, Blythe H J, Score D, Xu X H, Neal J R, Fox A M and Gehring G A 2008 *Phys. Rev. Lett.* **100** 047206
[24] Liu X X, Lin F T, Sun L L, Cheng W J, Ma X M and Shi W Z 2006 *Appl. Phys. Lett.* **88** 062508
[25] Park J H, Kim M G, Jang H M and Ryu S 2004 *Appl. Phys. Lett.* **84** 1338
[26] Coey J M D, Venkatesan M and Fitzgerald C B 2005 *Nature Mater.* **4** 173
[27] Fukumura T, Jin Z W, Kawasaki M, Shono T, Hasegawa T, Koshihara S and Koinuma H 2001 *Appl. Phys. Lett.* **78** 985
[28] Judith L, MacManus D, Neeraj K, Liu Y L and Mary E V 2006 *Adv. Mater.* **19** 2925
[29] Xu Q Y, Schmidt H, Hartmann L, Hochmuth H, Lorenz M, Setzer A, Esquinazi P, Meinecke C and Grundmann M 2007 *Appl. Phys. Lett.* **91** 092503
[30] Yan W S, Sun Z H, Liu Q H, Li Z G, Pan Z Y, Wang J, Wei S Q, Wang D, Zhou Y X and Zhang X Y 2007 *Appl. Phys. Lett.* **91** 062113
[31] Sluiter M H F, Kawazoe Y, Sharma P, Inoue A, Raju A R, Rout C and Waghmare U V 2005 *Phys. Rev. Lett.* **94** 187204